Nuclear quadrupole interactions of the ^{87}Rb nuclear magnetic resonance in a nonlinear optical crystal $RbTiOAsO_4$

2002 J. Phys.: Condens. Matter 14 13743

(http://iopscience.iop.org/0953-8984/14/50/303)

INSTITUTE OF PHYSICS PUBLISHING JOURNAL OF PHYSICS: CONDENSED MATTER

J. Phys.: Condens. Matter **14** (2002) 13743–13749 PII: S0953-8984(02)53432-9

Nuclear quadrupole interactions of the ^{87}Rb nuclear magnetic resonance in a nonlinear optical crystal $RbTiOAsO_4$

Ae Ran Lim[1,3], Hee Won Shin[1], Sooseok Lee[2] and Choon Sup Yoon[2]

[1] Department of Physics, Jeonju University, Jeonju 560-759, Korea
[2] Department of Physics, KAIST, Daeduck Science Town, Taejeon 305-701, Korea

E-mail: aeranlim@hanmail.net and ARL29@cornell.edu

Received 13 September 2002
Published 6 December 2002
Online at stacks.iop.org/JPhysCM/14/13743

Abstract

The ^{87}Rb nuclear magnetic resonance (NMR) in a $RbTiOAsO_4$ single crystal was investigated by employing a Bruker FT NMR spectrometer. Instead of one central line, four central lines were obtained. There were two sets of crystallographically inequivalent Rb^+ ions: Rb(1) and Rb(2). Two resonance lines in the Rb(1) nucleus and two resonance lines in the Rb(2) nucleus were caused by magnetically inequivalent sites. The angular dependences led to different values for the quadrupole coupling constant and the asymmetry parameter: $e^2qQ/h = 19.26 \pm 0.03$ MHz and $\eta = 0.59 \pm 0.02$ for the Rb(1) ion, and $e^2qQ/h = 23.58 \pm 0.07$ MHz and $\eta = 0.44 \pm 0.05$ for the Rb(2) ion. The EFG tensors of Rb(1) and Rb(2) were non-axially symmetric, and the orientations of their principal axes did not coincide. The Rb(1) ions, which are surrounded by nine oxygen atoms, are low in symmetry while the Rb(2) ions, which are surrounded by nine oxygen atoms, show high symmetry.

1. Introduction

Quasi-phase matching (QPM) provides an efficient way of effecting nonlinear frequency conversion and has a number of advantages over conventional birefringence phase matching because QPM not only can utilize the largest component of the second-order nonlinear susceptibility tensor but also can circumvent the walk-off effect [1]. A QPM structure can be realized by fabricating periodic domain inversion in ferroelectric nonlinear optical crystals, such as $LiNbO_3$ [2], $KTiOPO_4$ [3], and $RbTiOAsO_4$ [4]. Although $LiNbO_3$ has a large effective nonlinear optical coefficient of 17 pm V^{-1}, it has to be used at elevated temperatures because of the photorefractive effect at room temperature. $KTiOPO_4$ and $RbTiOAsO_4$ are free of the photorefractive effect and can be poled at thicknesses as large as 3 mm. However, since $KTiOPO_4$ has a

[3] Author to whom any correspondence should be addressed.

large electrical conductivity, electrical poling for domain inversion should be done at low temperature [3] or with K^+ ions replaced by Rb^+ ions [5] to reduce the conductivity. $RbTiOAsO_4$ is similar in structural and nonlinear optical properties to $KTiOPO_4$, but has an electrical conductively five orders of magnitude smaller than that of $KTiOPO_4$ [6] along the polar axis. $RbTiOAsO_4$ is, therefore, regarded as a promising material for QPM applications. Recently, Kaminsky *et al* [7] reported the measurement of optical rotation in $RbTiOAsO_4$ crystal.

The $RbTiOAsO_4$ crystal is a positive biaxial ferroelectric crystal belonging to the orthorhombic $Pna2_1(mm2)$ class [8], and its polar axis is parallel to its c-axis. $RbTiOAsO_4$ possesses excellent nonlinear optical properties, such as a wide transparency range in the IR region (0.35–5.3 μm) [9] and large second-order nonlinear optical coefficients ($d_{33} = 15.8$ pm V^{-1}, $d_{32} = 3.8$ pm V^{-1}, and $d_{31} = 2.3$ pm V^{-1}) [10]. Although its physical properties, such as its piezoelectric, acoustic [11], and dielectric properties [6], have been reported, no literature report has yet presented nuclear magnetic studies of $RbTiOAsO_4$.

In this paper, based on an investigation of the ^{87}Rb nuclear magnetic resonance (NMR) in a $RbTiOAsO_4$ single crystal, we discuss the local structure around the rubidium atoms. The quadrupole coupling constant, the asymmetry parameter, and the directions of the principal axes of the electric field gradient (EFG) tensor of ^{87}Rb ($I = 3/2$) were determined at room temperature. These results show that the crystallographically inequivalent Rb(1) and Rb(2) sites, which are surrounded by nine oxygen atoms each, can be clearly distinguished by means of the ^{87}Rb NMR.

2. Crystal structure

The structure for rubidium titanyl arsenate, $RbTiOAsO_4$, is orthorhombic with space group is $Pna2_1$ ($mm2$) [8]. There is no phase transition between room temperature and 9.6 K. The unit-cell parameters are $a = 13.218$ Å, $b = 6.6500$ Å, $c = 10.761$ Å, and $Z = 8$ at 9.6 K, and $a = 13.261$ Å, $b = 6.6791$ Å, $c = 10.769$ Å, and $Z = 8$ at 295 K [8]. The projection of the structure of $RbTiOAsO_4$ along [010] is shown in figure 1 [4]. As the temperature was lowered from 295 to 9.6 K, the Rb atoms moved along the c-axis in the direction of the polarization vector, while no significant change was noted for the Ti–O–As network. There are two types of crystallographically different Rb(1) and Rb(2), and As(1) and As(2) ions in the cell. The Rb^+ and As^+ ions are surrounded by oxygen atoms. Both Rb(1) and Rb(2) are located in channels along the c-axis and are coordinated by nine O atoms. The Rb–O bonds are longer in the positive than in the negative c-direction [12]. The Rb–O distances for Rb(1) and Rb(2) are given in table 1 [13].

3. Experimental details

Single crystals of $RbTiOAsO_4$ were grown by using the high-temperature solution growth method with a [001] seed placed at the surface of the solution [6]. The starting materials for the synthesis of $RbTiOAsO_4$ and a flux, $Rb_5As_3O_{10}$, were As_2O_5 (99.0% purity), TiO_2 (99.9% purity), and Rb_2CO_3 (99% purity). The weight ratio of $RbTiOAsO_4$ to the flux in solution was 3:10. $RbTiOAsO_4$ crystals, $18 \times 31 \times 24$ mm^3 in size and of excellent quality, were grown for a period of 25 days. The samples were cut and polished perpendicular to the three principal axes.

The NMR signals from ^{87}Rb in the $RbTiOAsO_4$ single crystals were measured using the Bruker DSX 400 FT NMR spectrometer at the Korea Basic Science Institute. The static magnetic field was 9.4 T, and the central radio-frequency was set at $\omega_0/2\pi = 130.930$ MHz. The angular variations of the spectra were obtained by rotating the crystal about three mutually

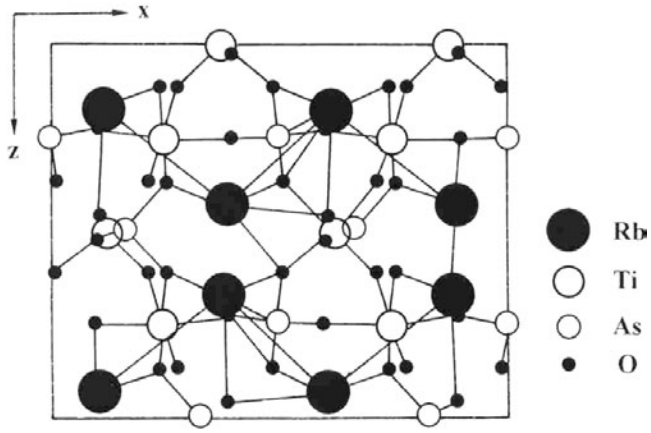

Figure 1. $RbTiOAsO_4$ crystal structure viewed along the [010] direction.

Table 1. Rb–O bond lengths for Rb(1) and Rb(2) in $RbTiOAsO_4$.

Bond type	Bond length (Å)	Bond type	Bond length (Å)
Rb(1)–O	3.145	Rb(2)–O	2.753
	2.808		3.109
	2.765		3.196
	3.297		3.030
	2.935		2.885
	3.017		3.183
	3.390		2.910
	3.307		3.002
	2.811		3.192
Average Rb(1)–O length: 3.053		Average Rb(2)–O length: 3.029	

perpendicular axes, which in turn were normal to the three mutually perpendicular planes of the crystal. A special probe head was constructed for the cryomagnet system, which rendered it possible to rotate the sample around an axis perpendicular to the static magnetic field $\boldsymbol{B}_0$ and to incline the complete probe head by angles up to about 5° with respect to the axis of the cryomagnet. Thus, the crystal orientation could be adjusted very sensitively with respect to the static magnetic field.

4. Experimental results and analysis

The NMR spectra of the ^{87}Rb nucleus were analysed using the usual Hamiltonian,

$$H = H_Z + H_Q, \tag{1}$$

where H_Z is the nuclear Zeeman term and H_Q describes the nuclear quadrupole interaction of the ^{87}Rb nucleus, which has a nuclear spin $I = 3/2$. The quadrupole Hamiltonian in the principal axis system of the EFG tensor is described by [14, 15]

$$\begin{aligned} H = -\gamma\hbar\boldsymbol{B}_0 \cdot (1+\boldsymbol{\alpha}) \cdot \boldsymbol{I} + [e^2 q Q/4I(2I-1)][\tfrac{1}{2}\{3I_z^2 - I(I+1)\}(3\cos^2\theta - 1) \\ + \eta \sin^2\theta \cos 2\varphi) + \tfrac{1}{4}(I_+^2 + I_-^2)\{3\sin^2\theta + \eta\cos 2\varphi(1+\cos^2\theta)\} \\ + \tfrac{1}{4}\{(I_+ + I_-)I_z + I_z(I_+ + I_-)\}(6\sin\theta\cos\theta - \eta\sin 2\theta\cos 2\varphi) \end{aligned}$$

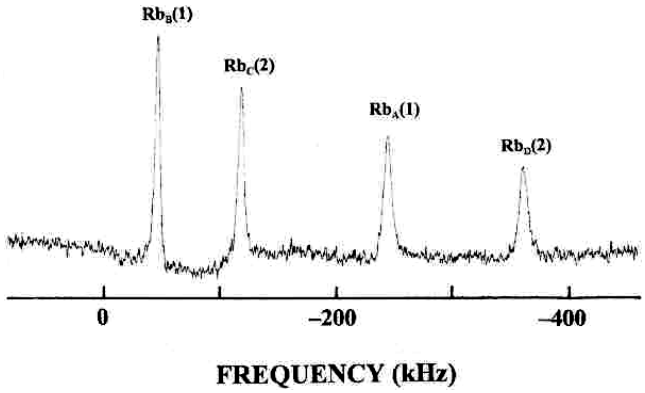

Figure 2. The NMR spectrum of ^{87}Rb in the $RbTiOAsO_4$ crystal. The static magnetic field B_0 is parallel to the $(b + 13°)$-axis in the ab-plane.

$$- (\eta/2\mathrm{i})(I_+^2 - I_-^2)\cos\theta \sin 2\varphi + \eta/2\mathrm{i}\{(I_+ - I_-)I_z + I_z(I_+ - I_-)\}\sin\theta \sin 2\varphi)], \quad (2)$$

where e^2qQ/h is the nuclear quadrupole coupling constant and η is the asymmetry parameter, α is the chemical shift tensor. The conventional X-, Y-, and Z-axes are such that $|V_{XX}| \leqslant |V_{YY}| \leqslant |V_{ZZ}| = eq$; then $0 \leqslant \eta \leqslant 1$. By using an EPR-NMR program which adopts the diagonalization algorithm for the matrix representation of the Hamiltonian instead of the perturbation method of Volkoff [16], we determined the nuclear quadrupole constant, the asymmetry parameter, and the principal directions of the EFG tensor.

The NMR spectra for ^{87}Rb in a $RbTiOAsO_4$ crystal at room temperature are shown in figure 2. The zero point in figure 2 corresponds to the resonance frequency of 130.930 MHz for the ^{87}Rb nucleus. Figure 2 represents the central transition $(\pm 1/2 \leftrightarrow \pm 1/2)$ of ^{87}Rb NMR. The satellite lines for the ^{87}Rb $(I = 3/2)$ nucleus, which correspond to the transitions $(+3/2 \leftrightarrow +1/2)$ and $(-1/2 \leftrightarrow -3/2)$, are out of range. When the crystal is rotated about the crystallographic axis, crystallographically equivalent nuclei give rise to three lines: one central line and two satellite lines. Instead of the one central resonance line of the ^{87}Rb nucleus, four central resonance lines are obtained in the case of the $RbTiOAsO_4$ crystal. This result points to the existence of two types of crystallographically inequivalent Rb nuclei, Rb(1) and Rb(2). The four central resonance lines correspond to two resonances in the Rb(1) nucleus and two resonances in the Rb(2) nucleus, all of which are caused by magnetically inequivalent sites. Figure 3 shows the angular dependence of the second-order quadrupole shifts of the ^{87}Rb resonance line in a $RbTiOAsO_4$ single crystal at room temperature. The dots correspond to the experimental values, and the full curves were obtained by fitting these data to symmetric second-rank EFG tensors. The rotation patterns indicate anisotropic EFG tensors. The Rb(1) nucleus shows a small deviation from the resonance frequency, but the Rb(2) nucleus has a largely deviation, as shown in figure 3. The deviations of these two groups, one smaller and the other larger, represent ^{87}Rb NMR transitions due to Rb(1) and Rb(2), respectively.

On the basis of the angular dependence of the second-order quadrupole shift in the central transition of the ^{87}Rb NMR, two different Rb resonance groups, which had different magnitudes for the quadrupole coupling constant and the asymmetry parameter, were analysed. In the case of $RbTiOAsO_4$, the maximum separation from the resonance frequency is about 600 MHz. Usually, the chemical shift is about 1–100 ppm [17]. The anisotropic chemical shift which is comparable to the second-order quadrupolar shift of the ^{87}Rb central transition

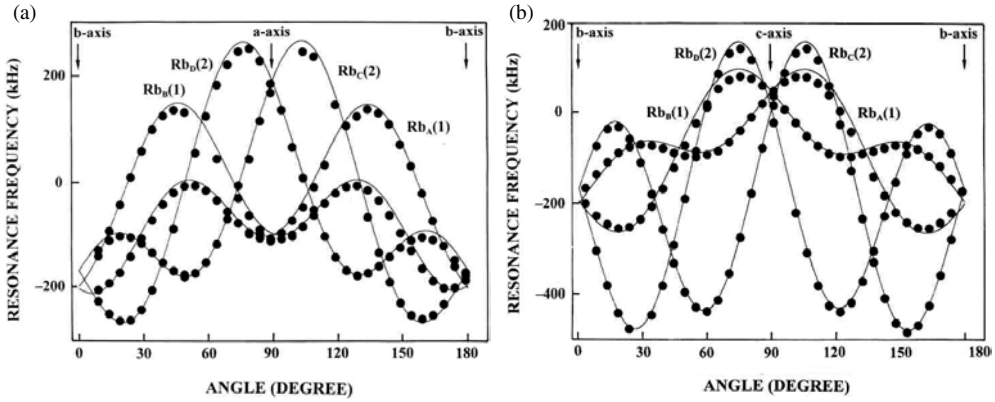

Figure 3. Rotation patterns of the Rb(1) and the Rb(2) NMR measured in the *ab*- and *bc*-planes at room temperature.

in a $RbTiOAsO_4$ single crystal is very small. The anisotropic chemical shift in this case is negligibly small [18]. Therefore, we have neglected the anisotropic chemical shift. Even if the anisotropic chemical shift is not considered, the NMR parameter is the same. The quadrupole coupling constant and the asymmetry parameter obtained for Rb(1), with the smaller deviation, are $e^2qQ/h = 19.26 \pm 0.03$ MHz and $\eta = 0.59 \pm 0.02$. Those for Rb(2), with the larger deviation, are $e^2qQ/h = 23.58 \pm 0.07$ MHz and $\eta = 0.44 \pm 0.05$. Therefore, the EFG tensors of Rb(1) and Rb(2) are not axially symmetric; the rubidium ions are surrounded by nine distorted oxygen atoms. The directions of the principal EFG tensors for the Rb(1) and the Rb(2) ions are shown in table 2. Where, $Rb_A(1)$ and $Rb_B(1)$, as shown in figure 3, are caused by magnetically inequivalent Rb(1) nuclei that are chemically equivalent. Also, in figure 3, $Rb_C(2)$ and $Rb_D(2)$ are split due to magnetically inequivalent Rb(2) nuclei that are also chemically equivalent. Here, μ_a, μ_b, and μ_c are the direction cosines relative to the crystallographic *a*-, *b*-, and *c*-axes of $RbTiOAsO_4$, respectively. The directions of the principal EFG tensors for the Rb ions are represented with the Eulerian angles $\Phi = 30.89°$, $\Theta = 79.31°$, and $\Psi = 45.05°$ for $Rb_A(1)$; $\Phi = 44.15°$, $\Theta = 79.46°$, and $\Psi = 44.92°$ for $Rb_B(1)$; $\Phi = 12.90°$, $\Theta = 74.79°$, and $\Psi = 166.07°$ for $Rb_C(2)$; $\Phi = 13.42°$, $\Theta = 74.97°$, and $\Psi = 14.34°$ for $Rb_D(2)$. The NMR parameters for the Rb(1) and the Rb(2) atoms are different. The nearest-neighbour Rb(1)–O bond lengths have an average of 3.053 Å while the Rb(2)–O bond lengths have an average of 3.029 Å. The Rb(2)–O bond is rather shorter than the Rb(1)–O bond lengths. Since the EFG is proportional to $1/r^3$ [19] and the asymmetry parameter represents the anisotropy of the EFG tensor, the Rb(1) site is expected to have a smaller e^2qQ/h and a larger η than the Rb(2) site.

5. Discussion and conclusions

The rotation patterns of the ^{87}Rb NMR in a $RbTiOAsO_4$ single crystal grown by using a high-temperature solution growth method were investigated in two mutually perpendicular crystal planes. Only four central lines were observed for each direction of the magnetic field. These four ^{87}Rb central lines showed the angular dependences of second-order quadrupolar shifts. From these angular dependences, all the parameters could be determined, leading to different values for the quadrupole coupling constant and the asymmetry parameter. The EFG tensors of Rb(1) and Rb(2) are both non-axially symmetric, and the orientations of the principal axes

Table 2. Direction cosines of the Rb(1) and the Rb(2) EFG tensors in $RbTiOAsO_4$.

	V_{XX}	V_{YY}	V_{ZZ}
$Rb_A(1)$			
μ_a	−0.67465	0.25087	0.69420
μ_b	−0.53884	0.47539	−0.69546
μ_c	0.50448	0.84325	0.18554
$Rb_B(1)$			
μ_a	−0.67770	0.24240	0.69423
μ_b	0.54664	−0.46540	0.69612
μ_c	0.49184	0.85126	0.18290
$Rb_C(2)$			
μ_a	−0.96021	0.15505	0.23226
μ_b	−0.17778	0.30194	−0.93660
μ_c	0.21539	0.94063	0.26235
$Rb_D(2)$			
μ_a	−0.95731	0.16239	0.23915
μ_b	0.18257	−0.30179	0.93573
μ_c	0.22413	0.93944	0.25925

of the EFG tensor do not coincide for the Rb(1) and the Rb(2) sites. There are two sets of crystallographically inequivalent Rb^+ ions, Rb(1) and Rb(2). Because Rb(2) is surrounded less symmetrically by nearer ligands than Rb(1), the quadrupole coupling constant of Rb(1) is smaller than that of Rb(2). The quadrupole coupling constant $e^2qQ/h = eQ(\partial E_z/\partial z)/h$ and asymmetry parameter $\eta = (\partial E_x/\partial x) - (\partial E_y/\partial y)/(\partial E_z/\partial z)$ for Rb(1) and Rb(2) can be calculated directly from the experimental data, but in order to obtain $eq = (\partial E_z/\partial z)$, one needs to know Q for the Rb nucleus. From these results, the components of the asymmetry parameter were found; the values for $|V_{XX}|, |V_{YY}|, |V_{ZZ}|$ are $1.26 \times 10^{21}, 4.88 \times 10^{21}, 6.14 \times 10^{21}$ V m^{-2} for Rb(1) and $2.10 \times 10^{21}, 5.41 \times 10^{21}, 7.51 \times 10^{21}$ V m^{-2} for Rb(2), respectively. We know that the Rb(2) ions surrounded by nine oxygen atoms have wider charge distributions than the Rb(1) ions surrounded by nine oxygen atoms. Thus, the quadrupole coupling constants and the asymmetry parameters of Rb(1) and Rb(2) reveal the configuration of ionic charges around Rb^+. The Rb(1) ions surrounded by nine oxygen atoms are lower in symmetry than the Rb(2) ions while the Rb(2) ions surrounded by nine oxygen atoms show high symmetry. Therefore, the Rb(1) and the Rb(2) atoms surrounded by nine oxygen atoms can be clearly distinguished from the ^{87}Rb NMR results.

Acknowledgment

This work was supported by grant No R05-2001-000-00148-0 from the basic research programme of the Korea Science and Engineering Foundation.

References

[1] Armstrong J A, Bloembergen N, Ducuing J and Pershan P S 1962 *Phys. Rev.* **127** 1918
[2] Shur V Y and Rumyantsev E L 1999 *Phys. Solid State* **41** 1681
[3] Rosenman G, Skliar A, Eger D, Oron M and Katz M 1998 *Appl. Phys. Lett.* **73** 3650
[4] Hu A W, Thomas P A, Webjorn J and Loiacono G M 1996 *J. Phys. D: Appl. Phys.* **29** 1681
[5] Karlsson H and Laurell F 1997 *Appl. Phys. Lett.* **71** 3474
[6] Yang Y and Yoon C S 1999 *Appl. Phys. Lett.* **75** 1164

[7] Kaminsky W, Thomas P A and Glazer A M 2002 *Z. Kristallogr.* **217** 1
[8] Thomas P A, Mayo S C and Watts B E 1992 *Acta Crystallogr.* B **48** 401
[9] Reid D T, Ebrahimzadeh M and Sibbett W 1995 *J. Opt. Soc. Am.* B **12** 2168
[10] Cheng L T, Cheng L K and Bierlein J D 1993 *Proc. SPIE* **1863** 43
[11] Chu D K T, Bierlein J D and Hunsperger R G 1992 *IEEE Trans. Ultrason. Ferroelectr. Freq. Control* **39** 683
[12] Almgren J, Streltsov V A, Sobolev A N, Figgis B N and Albertsson J 1999 *Acta Crystallogr.* B **55** 712
[13] El Haidouri A, Durand L and Cot L 1990 *Mater. Res. Bull.* **25** 1193
[14] Abragam A 1961 *The Principles of Nuclear Magnetism* (Oxford: Oxford University Press)
[15] Cowan B 1997 *Nuclear Magnetic Resonance and Relaxation* (Cambridge: Cambridge University Press)
[16] Volkoff G M 1953 *Can. J. Phys.* **31** 361
[17] Lim A R, Jeong D Y, Kim J H and Hahn J H 2001 *J. Phys.: Condens. Matter* **13** 2025
[18] Pole J A, Schneider W G and Bernstein H J 1959 *High Resolution Nuclear Magnetic Resonance* (New York: McGraw-Hill)
[19] Schumacher R T 1970 *Introduction to Magnetic Resonance* (New York: Benjamin)